Zeitschrift: Eclogae Geologicae Helvetiae
Herausgeber: Schweizerische Geologische Gesellschaft
Band: 83 (1990)
Heft: 3: The Hans Laubscher volume

Artikel: Kinematics and intrabed-strain in mesoscopically folded limestone layers : examples from the Jura and the Helvetic Zone of the Alps
Autor: Pfiffner, O. Adrian
DOI: https://doi.org/10.5169/seals-166603

Eclogae geol. Helv. 83/3: 585–602 (1990)

0012-9402/90/030585–18 $ 1.50 + 0.20/0
Birkhäuser Verlag, Basel

Kinematics and intrabed-strain in mesoscopically folded limestone layers: examples from the Jura and the Helvetic Zone of the Alps

By O. Adrian Pfiffner[1])

ABSTRACT

The uppermost Effingen Beds in the Jura Mountains consist of a rhythmic sequence of limestone beds separated by marl horizons. A detailed analysis at the outcrop scale in the core of the St. Sulpice anticline reveals that individual limestone layers maintain compatibility within the large scale structures by folding, bedding plane slip, conjugate contractional and extensional faults, and duplexes. The thickness of individual limestone layers appears not to be altered by a significant amount. Some of the contractional faults indicate considerable layer-parallel shortening in the early history of the folds. The ductile behavior indicated by round fold hinges is mainly linked to small scale faulting.

The "Mergelband" member in the Helvetic Zone of the Alps is a sequence of well-bedded limestones within the Late Jurassic Quinten Limestone. Within the anchizonal Helvetic Nappes individual limestone layers form chevron-type folds in the hinge of more concentric shaped large-scale folds. The strains necessary to produce the thickness variations and the round fold hinges were produced solely by fracturing and pressure solution. Material balancing in the hinge of a fold reveals a volume loss of about 23% due to pressure solution. Intrabed-strains related to buckling are of the tangential-longitudinal strain type. In particular there is no evidence for intracrystalline deformation under these metamorphic conditions.

The same "Mergelband" member in the epizonal Infrahelvetic complex is characterized by folds with extensive thickness variations in individual layers. Microstructural and textural analyses show that intracrystalline deformation was important and produced a strong shape-preferred orientation of the micritic grains, and also that a substantial amount of plastic flow post-dates the buckling stage of folding.

ZUSAMMENFASSUNG

Die oberen Effingerschichten im Jura bestehen aus einer Kalk-Mergel-Wechsellagerung, welche im Kern der Antiklinalen von St. Sulpice in Falten gelegt sind. Detaillierte Untersuchungen im Aufschlussbereich zeigen, dass die einzelnen Kalkbänke die durch die grossräumige Struktur bedingte Deformation durch Faltung, schichtparalleles Gleiten, konjugierte Aufschiebungen, Verwerfungen und Verschuppungen aufnehmen. Hierbei werden die Mächtigkeiten der einzelnen Kalkbänke nicht wesentlich verändert. Einige der Aufschiebungen deuten darauf hin, dass schichtparallele Verkürzung im frühen Stadium der Faltung stattfand. Das duktile Verhalten, angezeigt durch runde Faltenscharniere, kommt hauptsächlich durch kleinmassstäbliche Spröddeformation zustande.

Das «Mergelband» innerhalb des Quintnerkalks im Helvetikum besteht aus einer rhythmischen Abfolge von Kalkbänklein und leicht mergeligen Kalklagen. In den anchizonal überprägten Helvetischen Decken sind im Scharnier von grossräumigen Falten des Quintnerkalks im Mergelband mesoskopische, chevronartige Falten anzutreffen. Die für die Mächtigkeitsschwankungen nötigen Deformationen kamen dabei ausschliesslich durch Drucklösung und Sprödbruch zustande. Eine Massenbilanz im Scharnier einer Falte zeigt, dass durch Drucklösung ein Volumenverlust von etwa 23% resultierte. Die schichtinterne Kinematik einer gefalteten Kalkbank zeichnet sich durch schicht-

[1]) Geologisches Institut, Universität Bern, Baltzer-Strasse 1, 3012 Bern, Switzerland.

parallele Streckung im äusseren und schichtparallele Verkürzung im inneren Teil der Schicht aus. Intrakristalline Deformationen können nicht nachgewiesen werden.

Mesoskopische Falten im selben «Mergelband» im epimetamorph überprägten Infrahelvetikum zeigen bedeutende Mächtigkeitsunterschiede zwischen Schenkel und Scharnier einzelner Schichten. Mikroskopische Untersuchungen zeigen, dass intrakristalline Deformationen hier wichtig waren und zu einer deutlichen Formeinregelung der einzelnen Mineralkörner führte. Anzeichen für Spröddeformation fehlen. Zudem ergibt sich, dass die eigentliche Faltung von einer späteren homogenen Deformation vom Typ einfacher Scherung überprägt worden ist.

Introduction

Folding of sedimentary strata requires strains at scales smaller than the wavelength of the folds. These strains may occur within the folded layers and relate either to thickness variations between hinge and limbs or to the pattern of the intrabed kinematics such as tangential-longitudinal strain or flexural flow, as discussed in Ramsay (1967). In addition to intrabed-strain, layer-parallel slip may occur between layers and contribute to the solution of the room problem in fold cores pertinent to any folded medium.

When comparing the shape of folded layers, most structural geologists probably agree that fold shapes become rounder during deformation at higher temperature (e.g. under greenschist or amphibolite facies conditions) with important thickness variations for individual layers. Also one expects a switch in active deformation mechanism from predominantly brittle behavior in un- or weakly metamorphic terranes to viscous flow by inter- and intra-granular deformation mechanisms at higher temperatures.

The aim of this study is to analyse such changes quantitatively in folds affecting fine-grained micritic limestones under conditions ranging from very low metamorphism (diagenesis) to greenschist facies conditions. The samples are from the unmetamorphosed Jura Mountains and the anchi- to epizonal Helvetic Zone of the Central Alps.

Fold geometry, strain and deformation mechanisms

Jura Mountains

The Folded Jura forms an arcuate belt of folds that extends over a distance of 300 km. The folds consist of Mesozoic-Cenozoic cover sediments which are detached from the basement along a detachment located in middle or upper Triassic evaporites (see e.g. Laubscher 1977).

A series of folds affecting the early Late Jurassic Effingen Beds in the cluse de St. Sulpice (NE) at Les Prélaz (coord. 534.300/196.200) were examined in detail. The large-scale structural setting is given in Fig. 1 (see also Rickenbach 1925). The St. Sulpice anticline shows the typical features of Jura-type folds. The whole structure is assumed to be detached from the underlying basement along a Triassic evaporitic layer. Within the anticline, the upper Jurassic limestones represent the mechanically stiff member of the section and form box folds with relatively sharp kinks at the hinges. A folded thrust fault in the core of the anticline indicates layer-parallel shortening early in the deformation history. A thrust fault on the vertical southern limb on the other hand, is SE-vergent (i.e. "regard suisse") and developed at a later stage in the folding history.

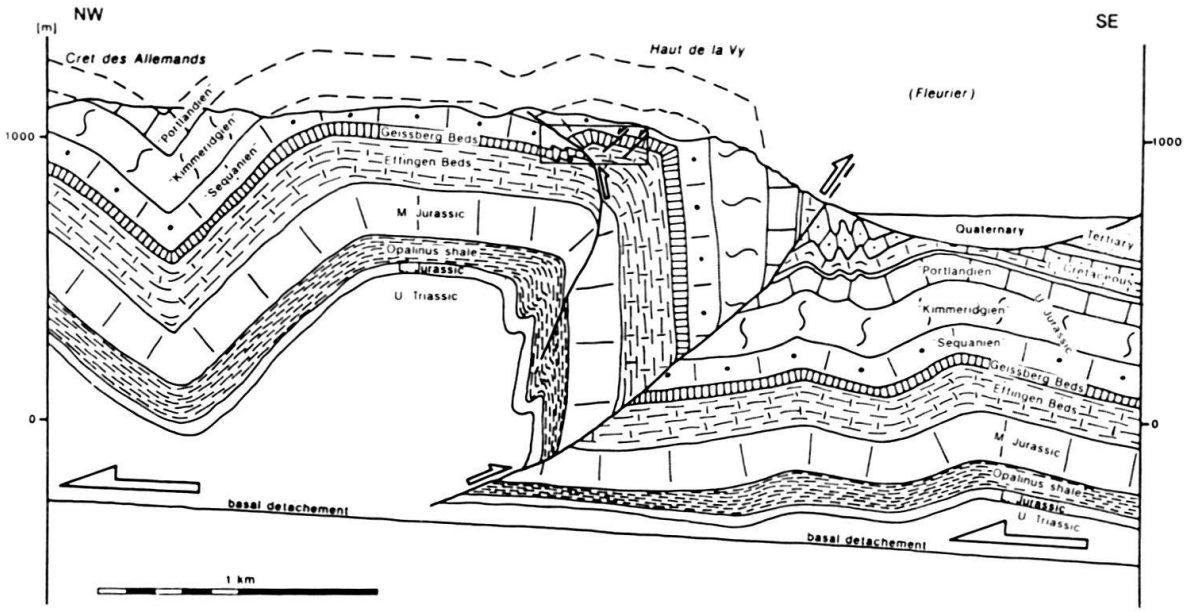

Fig. 1. Geologic profile through the St. Sulpice anticline in the Jura Mountains (W of Neuchâtel) showing the general structure. Rectangle shows location of Fig. 2.

Fig. 2 is a detailed picture of the structure around the folded thrust fault at the base of the mechanically stiff layer of Late Jurassic limestones. The conspicuous normal faults in the hanging-wall may be explained by layer-parallel extension within a hanging-wall anticline, which occurred during an early stage of the deformational history. In any case, the normal faults are unlikely to be related to the folding of the thrust fault because these normal faults are situated within the inner arc of the stiff layer. The folds in the more or less flat-lying layers of the footwall are interpreted as a collapse structure of a multilayer that underwent layer-parallel shortening, during the early stages of the deformational history.

Two areas within these folds were examined at the outcrop scale and are depicted in Figs. 3a and 3b. At both localities, the local stratigraphy of the individual limestone

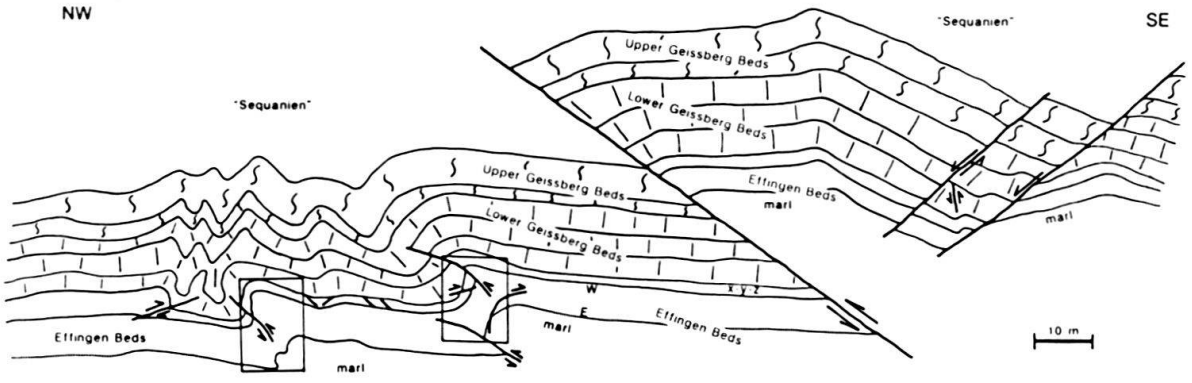

Fig. 2. Detailed cross section from Fig. 1, showing localised shortening under horizontal compression in the footwall. Rectangles mark location of Fig. 3 a), left and b) right. E, W and X-Y-Z refer to labels in Fig. 3.

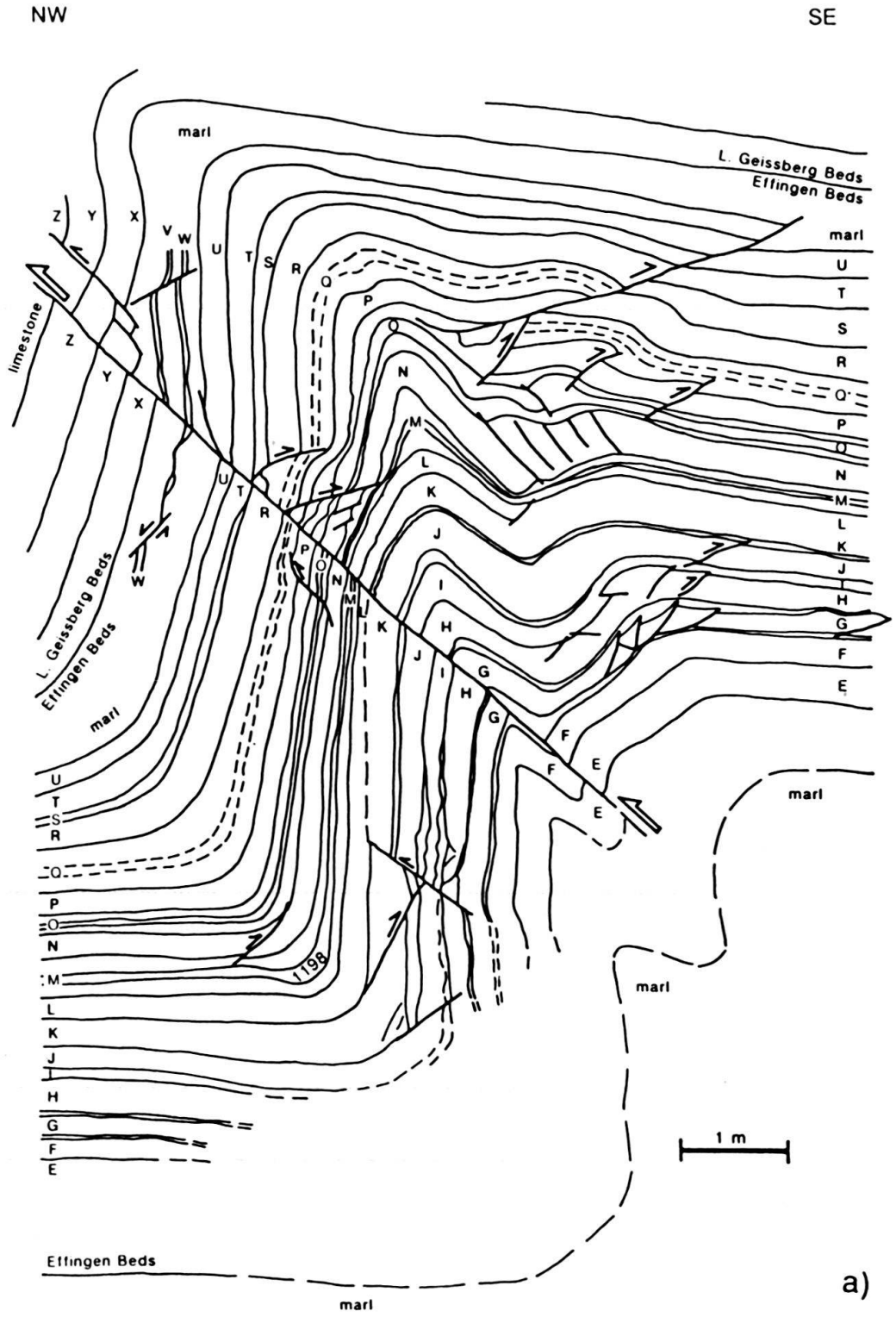

Fig. 3. Detailed cross sections from Fig. 2 (Les Prélaz) showing the complex interplay between folding and faulting. See text for discussion.

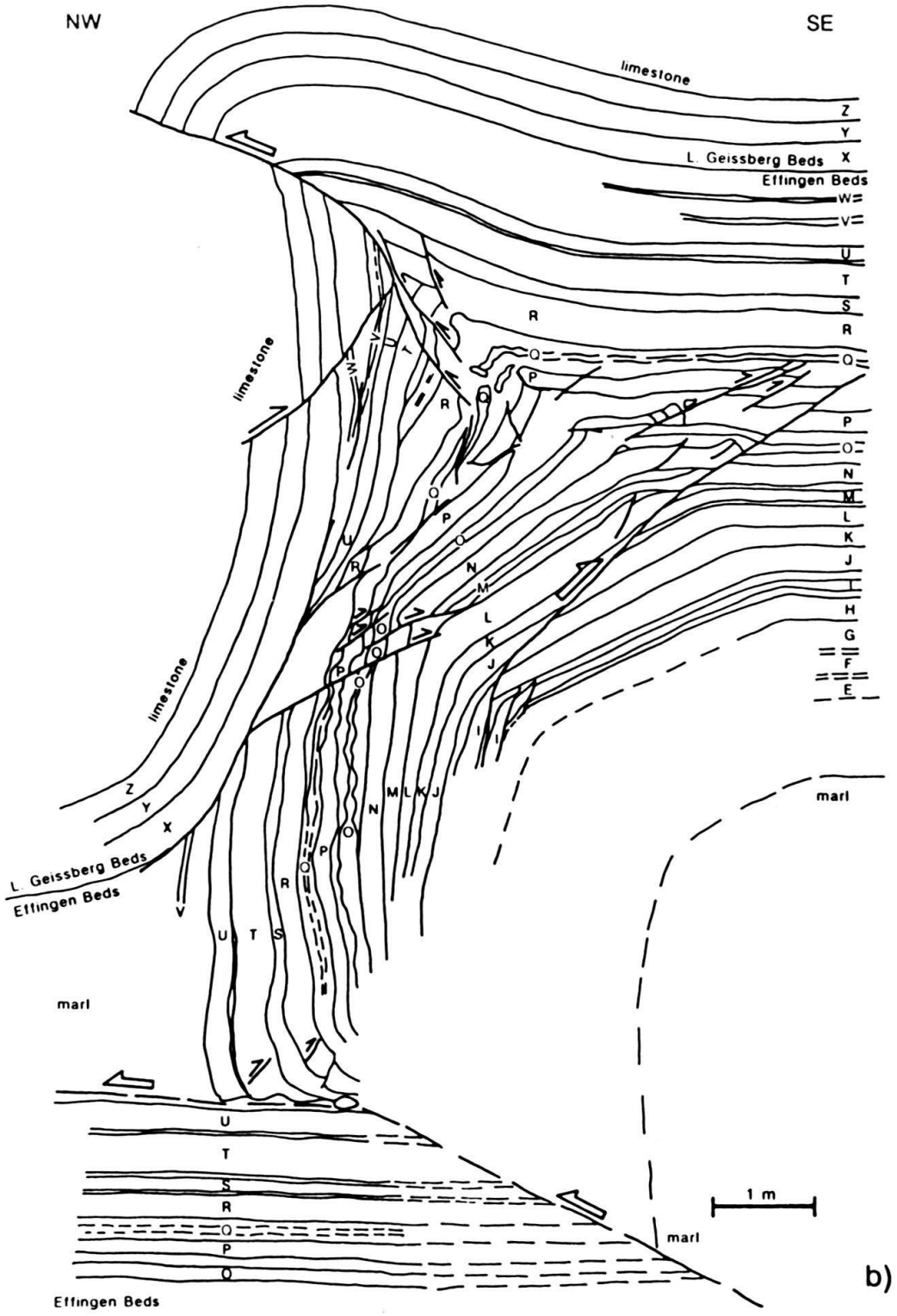
NW
SE
limestone
L. Geissberg Beds
Effingen Beds
marl
1 m
b)

layers is indicated by the labels E through Z. These limestone layers are separated by thin layers of marl. Based on a comparison of the thicknesses, it was possible to correlate the two sequences shown in Figs. 3a and 3b. Layers E through W represent the top of the Effingen Beds. These Effingen Beds form a predominantly marly sequence between Middle and Late Jurassic massive limestones. Layers X, Y and Z form the lowermost part of the Geissberg Beds, which are limestones that locally contain bioherms (PERSOZ & REMANE 1973) and lack bedding planes suitable for slip.

Inspection of the anticline-syncline pair in Fig. 3b reveals a complex interplay between faulting and folding. The structures are discussed by concentrating on the features encountered in following layer P through the folds. Beginning in the lower left, the abrupt change in orientation of bedding from horizontal to vertical is linked to a thrust fault which continues to the NE of the area shown in Fig. 3b. The displacement decreases along this fault because the thrust does not extend as far as the folds shown in Fig. 3a (cf. Fig. 2). The anticline-syncline pair of Fig. 3b is thus tentatively interpreted as a fault-propagation fold (SUPPE 1985 and SUPPE & MEDWEDEFF this volume). The vertical beds in the hanging-wall of this thrust fault are obviously thinned, as indicated by pinch-and-swell structures (layers O, P and Q), NW dipping reverse faults (stretching layer P as "normal faults" would do if P were horizontal) and discontinuous layers (U and V are cut off by X).

Layers I to Q are affected by several reverse faults, indicating layer-parallel shortening. For layer P, a pop-up structure bounded by two conjugate faults is situated immediately below the sharp kink in the anticline and indicates a vertical orientation of this shortening. This is probably unrelated to the later stages of buckling and closing of the fold. More likely it represents an early stage of layer-parallel shortening subsequently rotated into its present orientation.

Following layer P through the sharp kink to the SE several additional reverse faults document layer-parallel shortening or "wedging". Most of these faults do not extend into the adjacent limestone beds and must therefore transfer displacement into bedding-plane slip along the marly layers. The fault at the extreme right can be traced downwards into the core of the anticline where it is bent slightly between layers I and J. This suggests that it formed early in the folding history. Large-scale examples of folded and locked thrust faults are well known in the Jura Mountains through the pioneering work of BUXTORF (1916) in the Grenchenberg anticline (see also Fig. 1).

Folding within the Geissberg Beds is characterized by more rounded hinges (cf. Fig. 2), although thinning of the steep limb and closing of the anticline in Fig. 3b was accomplished by faulting in the lowermost beds (X, Y and Z).

The anticline-syncline pair in Fig. 3a shows similar features. Tracing limestone layer P through the structure reveals a rounded hinge in the syncline, layer-parallel extension in the steep limb (probably related to the actual folding process) and several reverse faults indicating layer-parallel shortening. The latter may have formed at early stages within the folding history. One of the reverse faults in the SE limb of the anticline truncates several beds (P–U) and may be due to squeezing material out of the fold core.

The conspicuous SE-dipping reverse fault cross-cutting the entire limb is obviously a late feature. Between layers F and G, this fault occurred within the suitably oriented marly layer. Its displacement of layers E and X is about the same, but straining within

the wall rocks decreased the displacement of layers P to U. The geometry in Fig. 2 indicates that the displacement on this reverse fault is transferred to folding in the layers of the Geissberg Beds above, and that the reverse fault is related to a late stage of tightening of those folds.

The hanging-wall rocks of the reverse fault in Fig. 3a exhibit three different structural styles:

– Layers G and H are folded and conjugate reverse faulting or "wedging" seems to be particularly important in the hinge zones of the folds (the same is true for layers I, M, N and O in the folds of Fig. 3b).

– Layer N accommodated some of the equivalent shortening mainly by NW-directed imbricate thrusting. The relatively thick marly layers below and above N facilitated the development of a duplex structure.

– Layer P shows SE-directed imbricate thrusting. The complex structure of layer O accounts for the kinematic consequences of the opposing movement directions above and below.

The fact that these different structural styles account for the equivalent strain in different layers suggests that folding and faulting were coeval.

It is generally assumed that the principal shortening direction in folds of the type described here is perpendicular to the fold axis. This assumption can be tested here by comparing the orientation of the fold axis as determined from bedding plane poles and the paleo-stress axes determined from faults with slickensides.

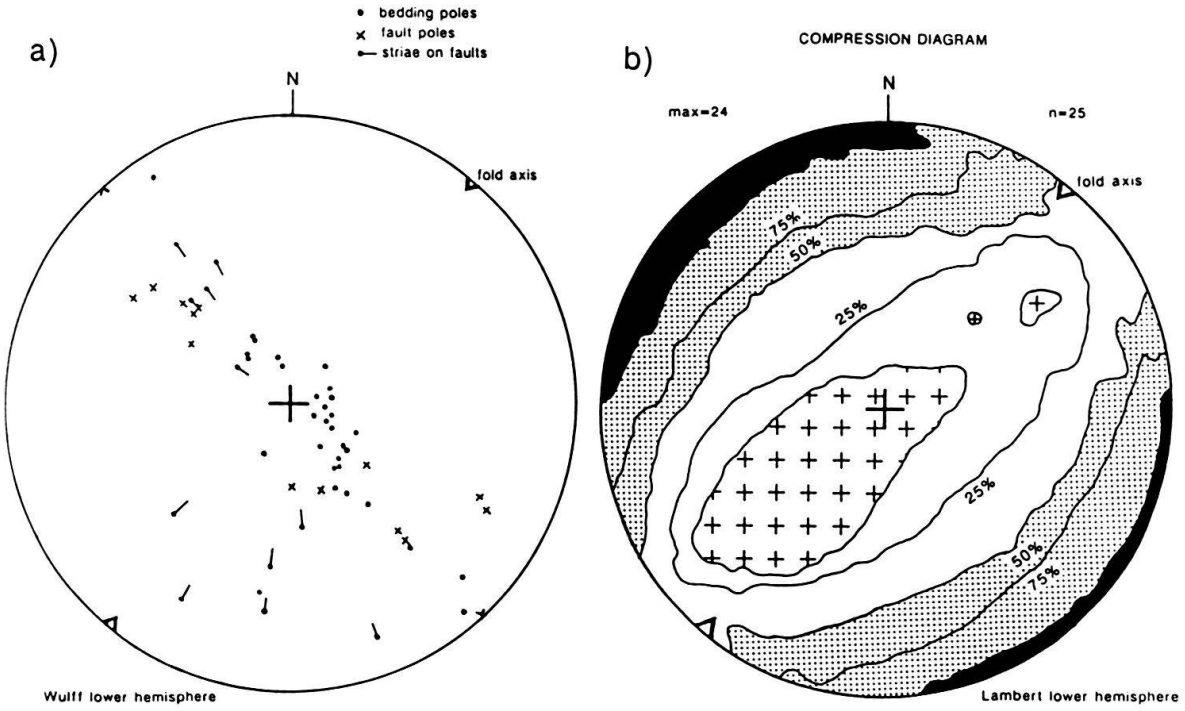

Fig. 4. Stereoplots of the folds of Fig. 3. a) poles to bedding and faults plot on a great circle which defines the fold axis. b) Contour diagram of possible paleostress-axes orientations. Black = 100%, stippled = 50–99%, white = 0–49% for σ_1 (maximum compression). Crosses: 100% for σ_3.

The internal structure of the folds shown in Figs. 3a and 3b is characterized by various faults and seems complex at first sight. Striations and slickensides on these faults suggest that some movement in and out of the profile plane did occur. Nevertheless the folds seem to be remarkably cylindrical as indicated by the dispersion of the poles to bedding and faults on a great circle in the stereogram shown in Fig. 4a. As described above, faulting may precede folding (layer-parallel shortening), be coeval with folding, or in some cases, even post-date folding. The position of the paleostress axes for each individual fault can be constrained by using faults with striae and known sense of slip. After a method outlined by ANGELIER (1977) and PFIFFNER & BURKHARD (1987), data sets consisting of many striated faults can be combined, assumed to a first approximation that all striated faults developed under a common stress field. Obviously, this assumption is not strictly tenable because some of the faults are early and are related to layer-parallel shortening in the rotated, steep limbs of Figs. 3a and b. Disregarding the faults from the steep rotated fold limbs, the resulting compression diagram (shown in Fig. 4b) suggests that the maximum compression axes σ_1 was subhorizontal and in a NW-SE direction. The paleostress axes thus indicate a shortening direction which is in fact compatible with the shortening direction inferred from the fold axis. For the minimum compression axis σ_3, a field extending from a subvertical to a shallow dipping NE-SW trending position emerges. The fact that 24 out of 25 data

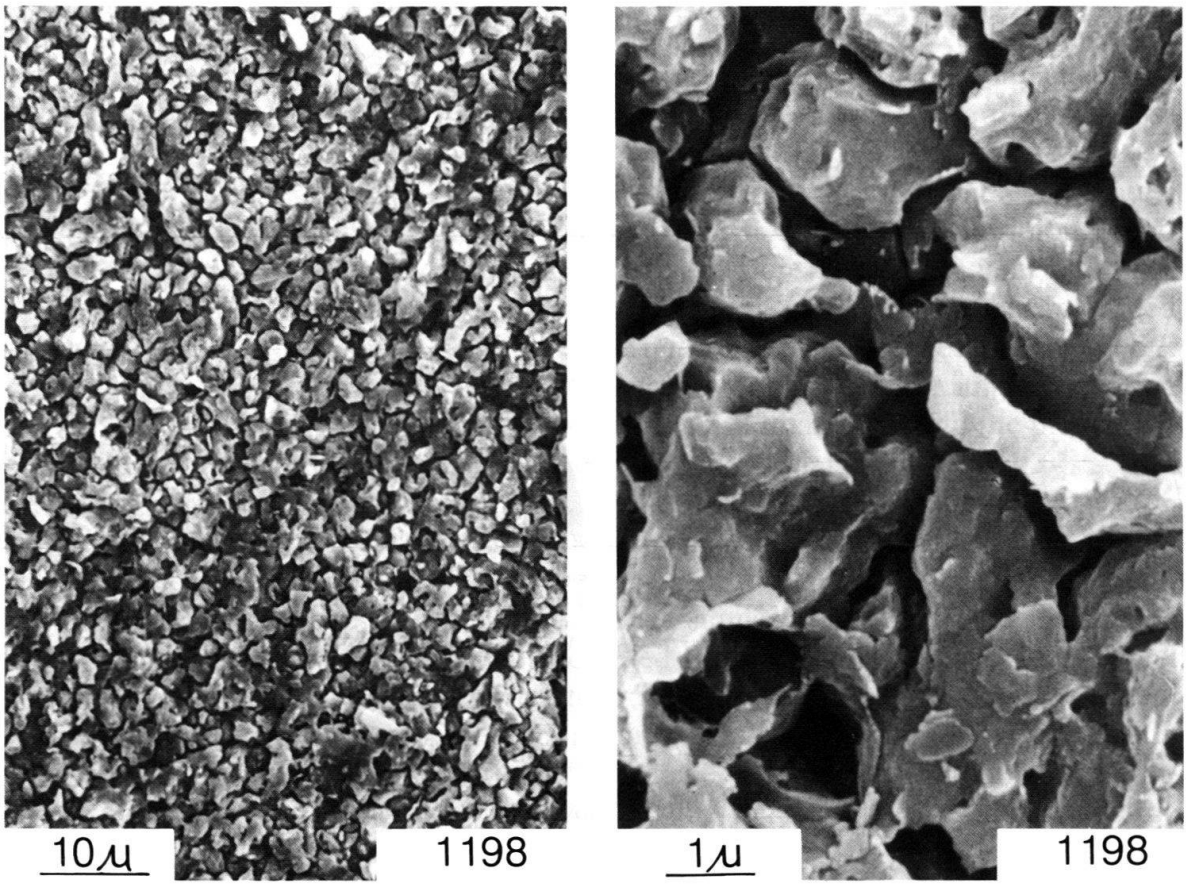

Fig. 5. SEM micrographs obtained from etched polished surfaces showing typical microstructure of sample 1198 from the unmetamorphic Jura Mountains.

sets are compatible with this position of the σ_1-axis and that a large area with a zero occupation density for the σ_1-axis exists suggests that the data set is coherent (internally consistent) and that the interpretation is reliable (see PFIFFNER & BURKHARD 1987 for a detailed discussion).

One of the aims of the study was to determine the deformation mechanisms at small scales. Since transmission optical microscopy is difficult to apply to these micritic limestones, scanning electron microscopy of etched surfaces was used to study grain shape fabrics. Sample 1198 shown in Fig. 5 was taken from the hinge of a syncline (cf. Fig. 3a, layer M). The lack of a grain shape fabric speaks against any significant intracrystalline deformation.

Field inspection, however, clearly indicates penetrative deformation at the cm scale by means of numerous striated and highly curved faults, which are best observed on fresh, broken surfaces of hand specimen. These faults are obviously responsible for the accomodation of local strains and rotations in conjunction with bending and thickness changes of individual limestone layers. Stylolites, particularly common in the oolitic limestones in the Jura mountains, were very rarely observed in the outcrops analysed. Veins filled with secondary calcite are also relatively scarce and occur in the highly deformed areas (e.g. the wedges defined by layer O in Fig. 3b).

In summary, the strains associated with the ductile folding in the unmetamorphic Jura Mountains were accommodated mainly by faulting at scales smaller than the observed folds. For folds at the outcrop scale, this includes combined reverse and normal faults. In smaller scale folds affecting individual limestone layers, curved striated faults facilitated block rotations in fold hinges and also account for thickness variations on fold limbs.

Helvetic Nappes

The Helvetic Zone of the Alps of eastern Switzerland is subdivided by the Glarus thrust into the Helvetic Nappes proper overlying this thrust fault and the underlying Infrahelvetic complex. The Helvetic Nappes represent a fold-and-thrust belt with an important detachment horizon, the Säntis thrust, in the lowermost Cretaceous shales. Beneath the Säntis thrust the internal nappe structure is dominated by the approximately 500 m thick Late Jurassic Quinten Limestone, which represents the mechanically stiff layer (see PFIFFNER 1981 and reference therein for a more detailed description). The folds analysed here are second order folds from the hinge zone of a major fold (cf. Fig. 6) collected near the village of Mäls (Liechtenstein, coord. 754.800/213.300). They occur in the "Mergelband", a well-bedded 30 m thick sequence consisting of 5–20 cm thick micritic limestone beds alternating with 1–3 cm thick layers of very calcareous marl.

Sample 1072 is the hinge of a syncline (see Fig. 6, inset) and its shape approximates that of a similar fold. The sample was cut into slices and analysed on polished surfaces. It is depicted as an antiform in Figs. 7 and 8 for reasons of convenience. The dominant deformational features are tension gashes concentrated in the outer part of the folded layer and stylolites in the inner part (Fig. 7a). In order to gain insight into the intrabed-strain necessary to produce a nearly similar fold with important thickness variations between limbs and hinge, a paper copy of the fold was cut along the interfaces between

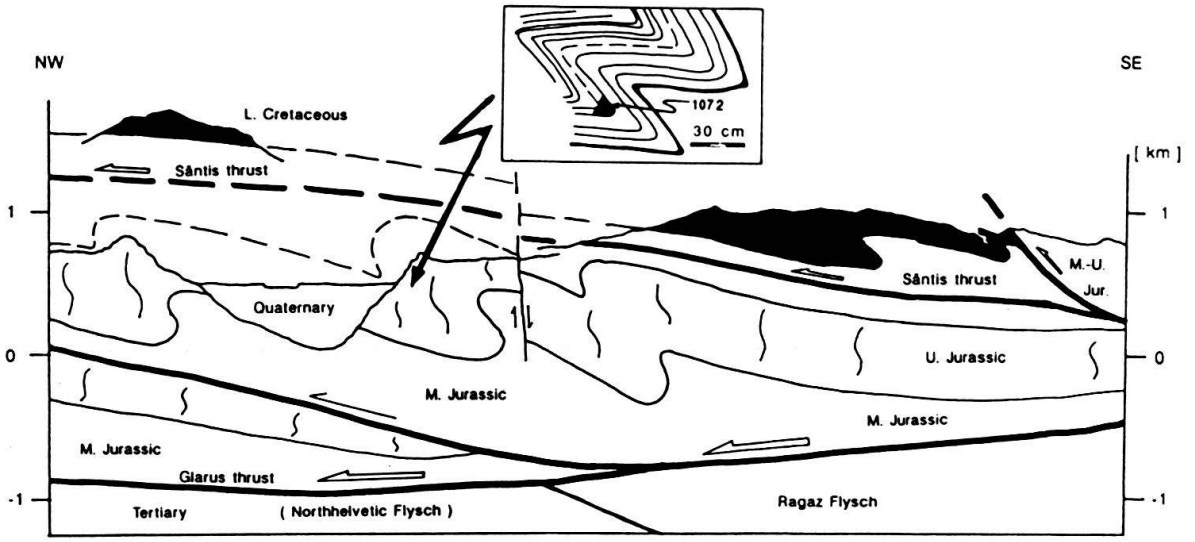

Fig. 6. Geologic profile showing the general structure of the Helvetic Nappes of eastern Switzerland (south of Liechtenstein). Inset: location of fold sample 1072 in the hinge of a syncline.

rock and secondary calcite vein filling, as well as along the observed stylolites. The resulting puzzle consisting of fragments of "rock" was reconstructed (or "retrodeformed") so that the bedding planes bounding the folded layer were as straight as possible. A minimum estimate of the layer thickness was obtained from the retrodeformed pieces making up the fold hinge. The fragments separated by veins in the deformed state generally fitted together neatly. The openings along the stylolites turned out to be significant in many instances. They are indicated in black in the retrodeformed state shown in Fig. 7b. Some of the thin veins in the deformed state turned out to be late openings along pre-existing stylolites, i.e., the bulk of the retrodeformation implied drifting apart of the pieces rather than closing of the (narrow) gap. This type of fracturing along stylolitic joints has been described in folds of the Jura Mountains (Droxler & Schaer 1979).

A mass balance between dissolved and reprecipitated calcite taking as a reference state the retrodeformed "volume" (black plus white area in Fig. 7b) reveals the following: 35.6% of the original rock volume was dissolved, but only 12.6% of the original volume was reprecipitated in the veins of the deformed state (the deformed state, i.e. black plus white in Fig. 7b), makes up only 76.9% of the reference state). This means that 23.1% of the rock volume was lost from the system in the folding process. This is probably a slight overestimate because pore space was reduced during this same stage. However, porosity of these micrites at the onset of folding was probably of the order of a few percent only (Moore 1989).

By comparing positions of individual "rock" fragments between the deformed and retrodeformed state, it is possible to determine the state of strain. After a method described by Ramsay (1967, p. 80 construction 4), triangles linking fragment centers (dots in Fig. 7) on the two limbs and in the inner and outer layer of the hinge were analysed. The resulting strain ellipses are given in Fig. 8a. The four triangles were chosen such that they have at least one side parallel to a straight bedding plane segment. This

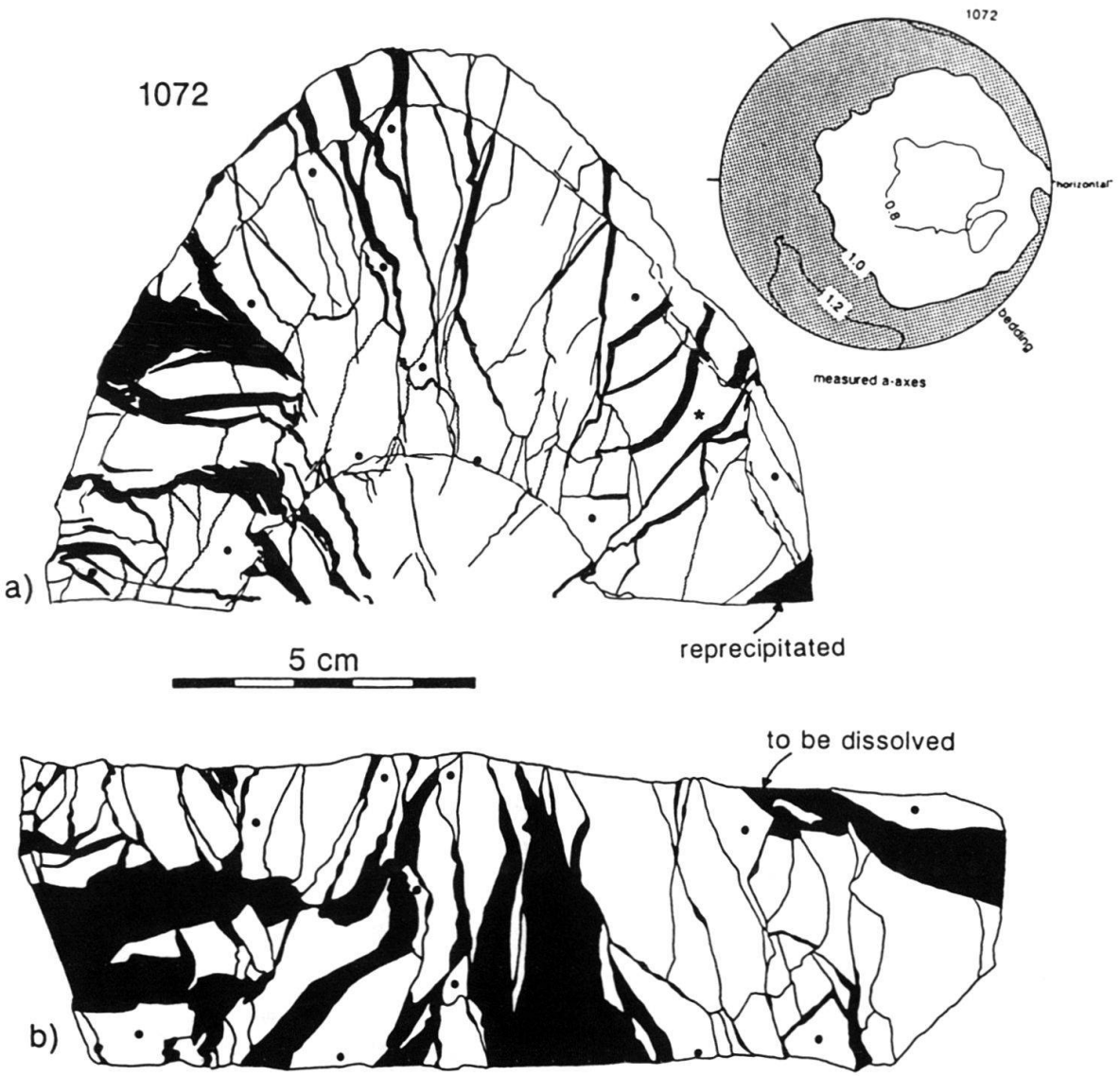

Fig. 7. Deformed (observed) and retrodeformed (reconstructed) state of sample 1072. Dots mark reference grid used in the strain study. Star: location of sample texture shown above. a) Fold profile of sample 1072. Note wedge-shaped veins (black) indicating extension in the outer arc and stylolites (wiggly traces) in inner arc and on limbs. b) Retrodeformed state. Note large "openings" (black) in the future inner arc and on limbs representing material which was dissolved.

guarantees that the strain ellipses are the result of a homogeneous deformation, which requires that straight lines before deformation remain straight after deformation. The long axis of the strain ellipse in the inner layer of the hinge is oriented oblique to the axial surface of the fold. This stems mainly from the fact that during the "retrodeformation" the fragment containing the apex of the triangle was not moved past the lozenge-shaped fragment above because of mutual interference. If these fragments were allowed to slide past each other (by movements in and out of the profile plane) the resulting strain ellipse would come to lie with its long axes in the axial plane. In either case, the strain in the hinge zone suggests that tangential-longitudinal strain was the

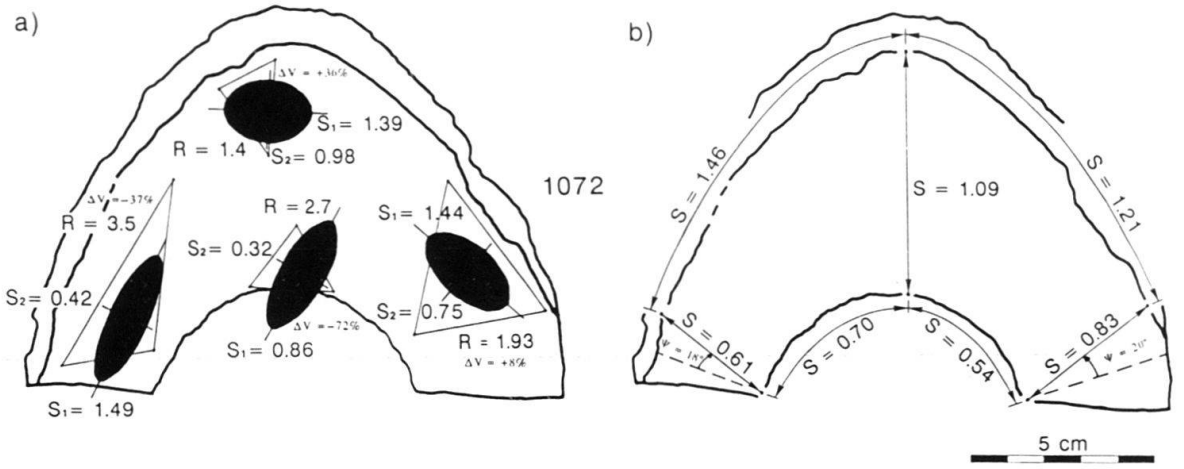

Fig. 8. Strain data for fold shown in Fig. 6a. a) Strain ellipses calculated from deformed and retrodeformed triangles. S_2 and S_1: lengths of long and short axes of strain ellipse expressed as stretch ($S = 1 + \Delta l/l_0$). ΔV: volume change (positive for increase). b) Thickness variations and layer-parallel deformation expressed as stretch. Ψ: angular shear of line initially orthogonal to bedding.

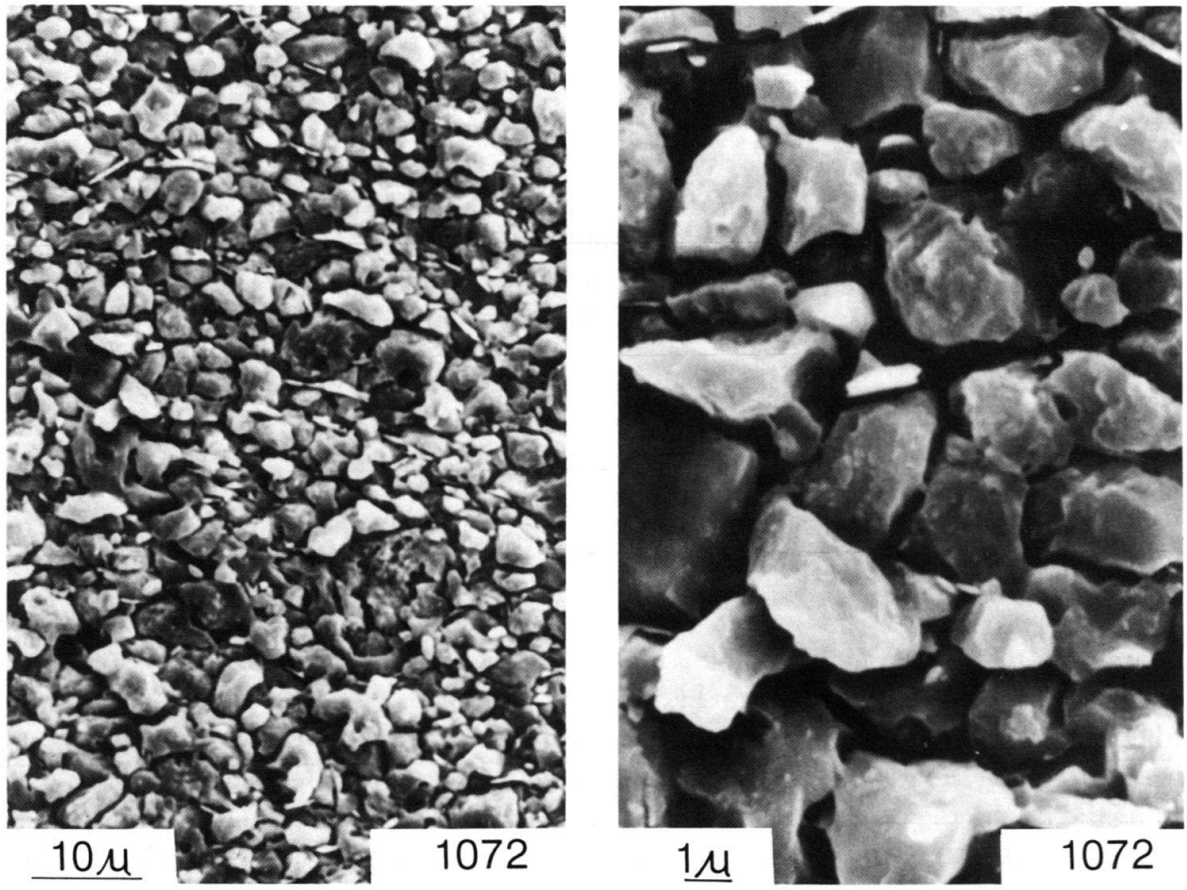

Fig. 9. SEM micrographs obtained from etched polished surfaces showing typical microstructure of sample 1072 from the anchimetamorphic Helvetic Nappes.

dominant pattern of intrabed kinematics, with bedding-parallel extension ($S_1 = 1.39$) in the outer, and shortening in the inner layer ($S_2 = 0.32$) in Fig. 8a.

Shape and orientation of the strain ellipses on the limbs document thickness variations that are largely due to thinning of the limbs. Bulk values of stretch parallel and perpendicular to bedding were determined and are presented on Fig. 8b. These values support the notion that thickness changes are due more to thinning of the limbs than to thickening in the hinge. This is supported by field observation of a set of stylolites oriented parallel to the axial surface indicating layer-parallel shortening (i.e. no thickness change) in the hinge. On the limbs, where the stylolites are at a shallow angle to bedding, the beds were thinned.

In order to detect intracrystalline deformation features several samples from fold 1072 were analysed on the texture goniometer. These samples all yielded an extremely weak crystallographic preferred orientation. The inset in Fig. 7a is a stereogram of the measured a-axes as determined on the rock fragment marked with a star in the right limb. The data are rotated into the orientation of Fig. 7a of the fold and the contours, given as multiples of uniform (see Schmid et al. 1987), reveal a lack of any significant texture. Similarly the SEM micrographs of etched surfaces on sample 1072 shown in Fig. 9 show that no shape preferred orientation exists. Therefore intracrystalline deformation mechanisms were not activated substantially during folding and most of the strain was accommodated by pressure solution and fracturing. Transmission optical microscopy reveals that the sparry vein filling was subjected to some mechanical twinning in a later stage.

Infrahelvetic complex

The Infrahelvetic complex comprises all units underlying the basal Glarus thrust of the Helvetic Nappes (Milnes & Pfiffner 1977, Pfiffner 1978). This complex forms a thick-skinned fold-and-thrust belt of its own, with basement rocks of the Aar massif forming the core of the major structures (Pfiffner et al. 1990). The general structure is characterized by a ductile deformational style leading to large-scale folds with inverted limbs (see Fig. 10) and smaller-scale parasitic folds. The Mesozoic rocks involved are similar to the ones in the Helvetic Nappes, but underwent an epizonal (greenschist facies) metamorphism. Growth of chloritoid related to this metamorphism post-dates cleavage formation associated with the main phase of deformation (named Calanda phase by Milnes & Pfiffner 1977, Pfiffner 1978). Thus metamorphism outlasted the deformation which was responsible for the folds analysed in this study.

Sample 1088 is from the hinge of a large-scale anticline (Fig. 10) and was collected near the village of Felsberg (coord. 754.850/191.400). The sample is actually from the same "Mergelband" as sample 1072. These Late Jurassic limestones form a number of tight folds encompassing a sequence reaching from upper Paleozoic volcanics into upper Cretaceous limestones (Fig. 10). The Cretaceous limestones were not detached from the upper Jurassic limestones as in the case of the Helvetic Nappes in the previously discussed folds. Rather, the entire sequence of Mesozoic carbonates form the mechanically stiff layer. The folds of sample 1088 were collected from the middle of this sequence.

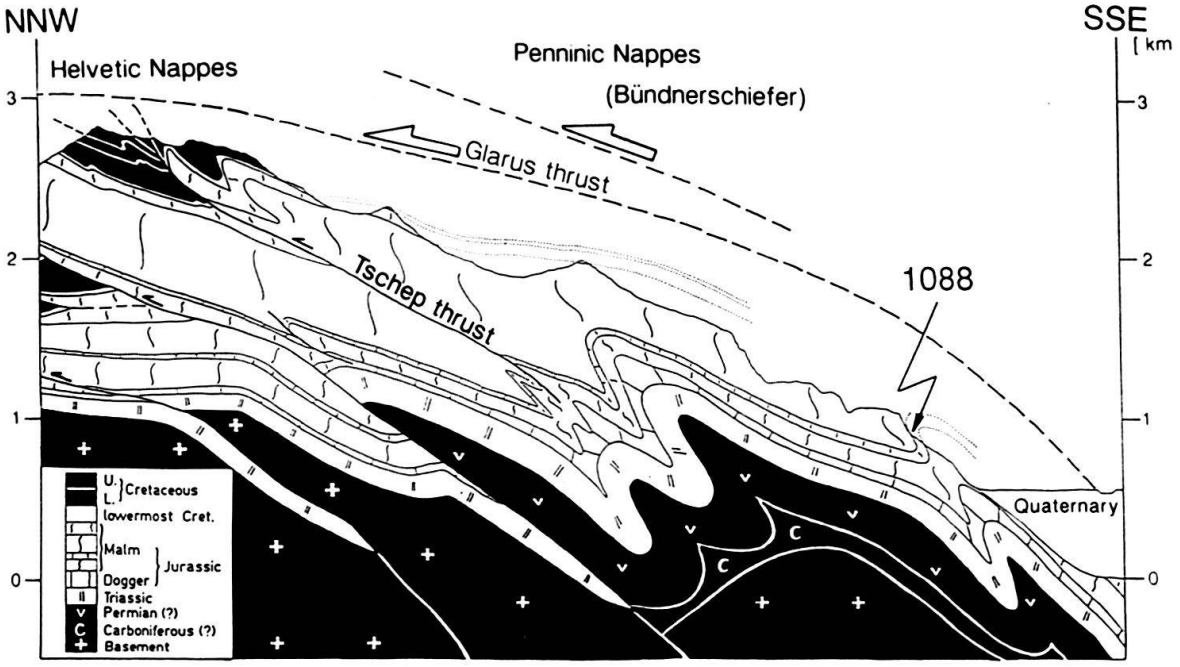

Fig. 10. Geologic profile of the Infrahelvetic complex in eastern Switzerland (N of Chur) showing the general structure and location of sample 1088.

Fig. 11 shows that folding lead to important thickness variations. Polyharmonic folding is quite common and indicates ductile flow throughout the folding history. A penetrative axial planar foliation forms convergent and divergent cleavage fans. Microscopically, the foliation is defined by a pronounced grain shape fabric (Fig. 12). The asymmetry of the large-scale structures suggests that the folds underwent a NNW directed sinistral shear, which is also in agreement with a regional, down-dip stretching lineation on cleavage planes (Pfiffner 1978, 1980). The folds shown in Fig. 11 lack any sign of imbricate thrusting related to layer-parallel shortening, stylolites or fracturing and veins. It thus seems that these folds formed directly as a result of ductile deformation, when the rocks were deeply buried. A similar scenario has been proposed from an attempt to relate the orogenic evolution of the Helvetic Zone with the development of the North-Alpine foreland basin (Pfiffner 1986). The Helvetic Zone seems to have evolved by a progression of thrusting from top to bottom with the internal deformation of the Infrahelvetic complex occurring later than the internal deformation of the Helvetic Nappes.

In order to determine intracrystalline deformation mechanisms, microscope and texture goniometer investigations were carried out. In Fig. 12, micrographs of etched surfaces as seen on a scanning electron microscope show a pronounced shape preferred orientation. The calcite grains are elongate and the grain boundaries are straight. This microstructure and the associated subgrains are both consistent with plastic flow by dislocation creep. The microstructure is slightly annealed, as seen in other rocks from the same general area (Pfiffner 1982).

The crystallographic preferred orientation was measured at the sites A through I in sample 1088 (Fig. 11) in order to relate texture types and asymmetry to the intrabed

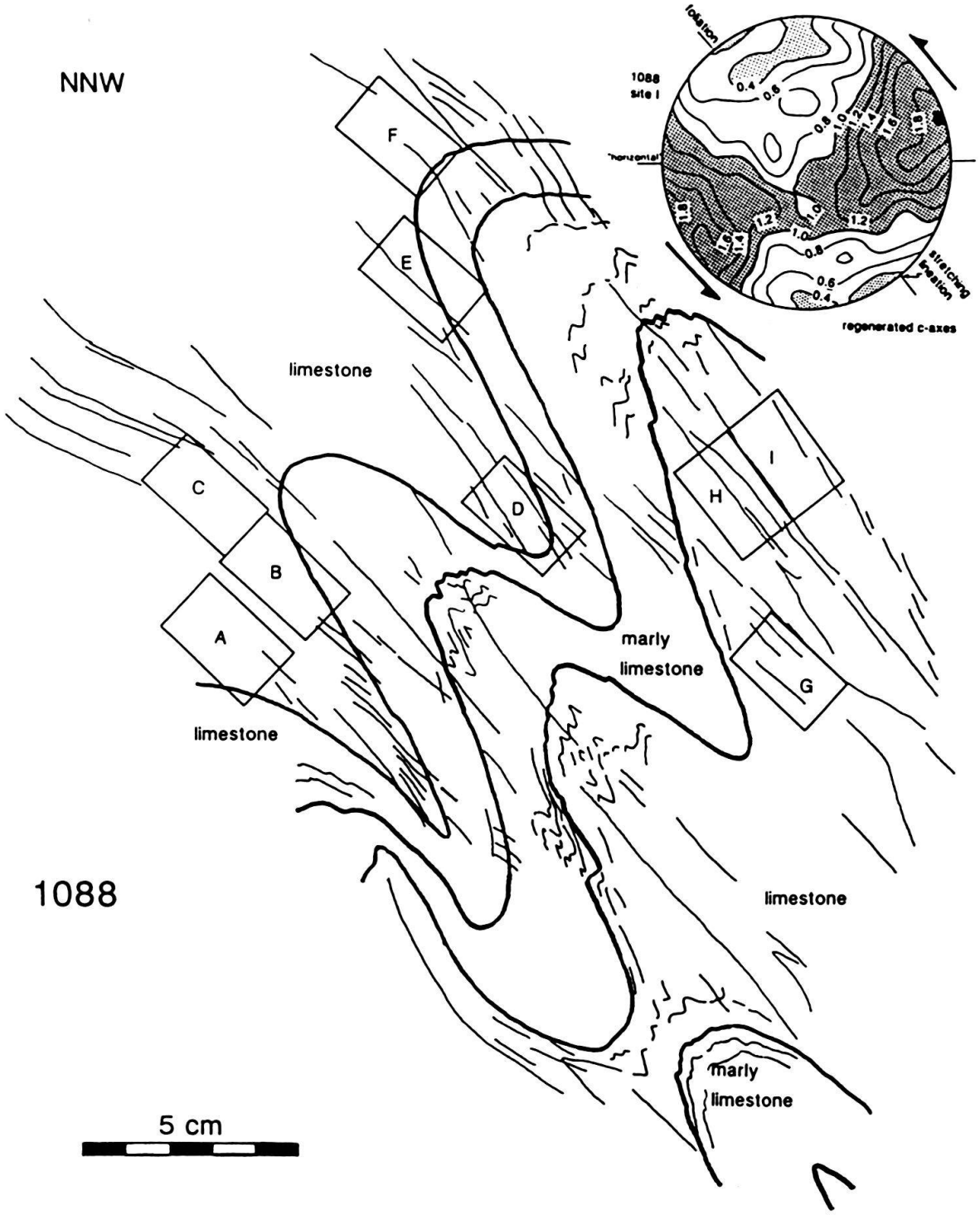

Fig. 11. Detailed cross section of the folds of sample 1088. Fine lines are cleavage traces. Rectangles A–I show location of thin sections for which texture analyses were carried out and of which only the one from site I is reproduced here. Arrows next to the stereoplot give sense of shear indicated by obliquity of c-axes maximum.

kinematics. Surprisingly, all the textures are more or less identical in terms of their intensity and their asymmetry with respect to the axial plane of the fold. Therefore, only the stereoplot of the regenerated c-axes at site I is given in Fig. 11. The c-axes show

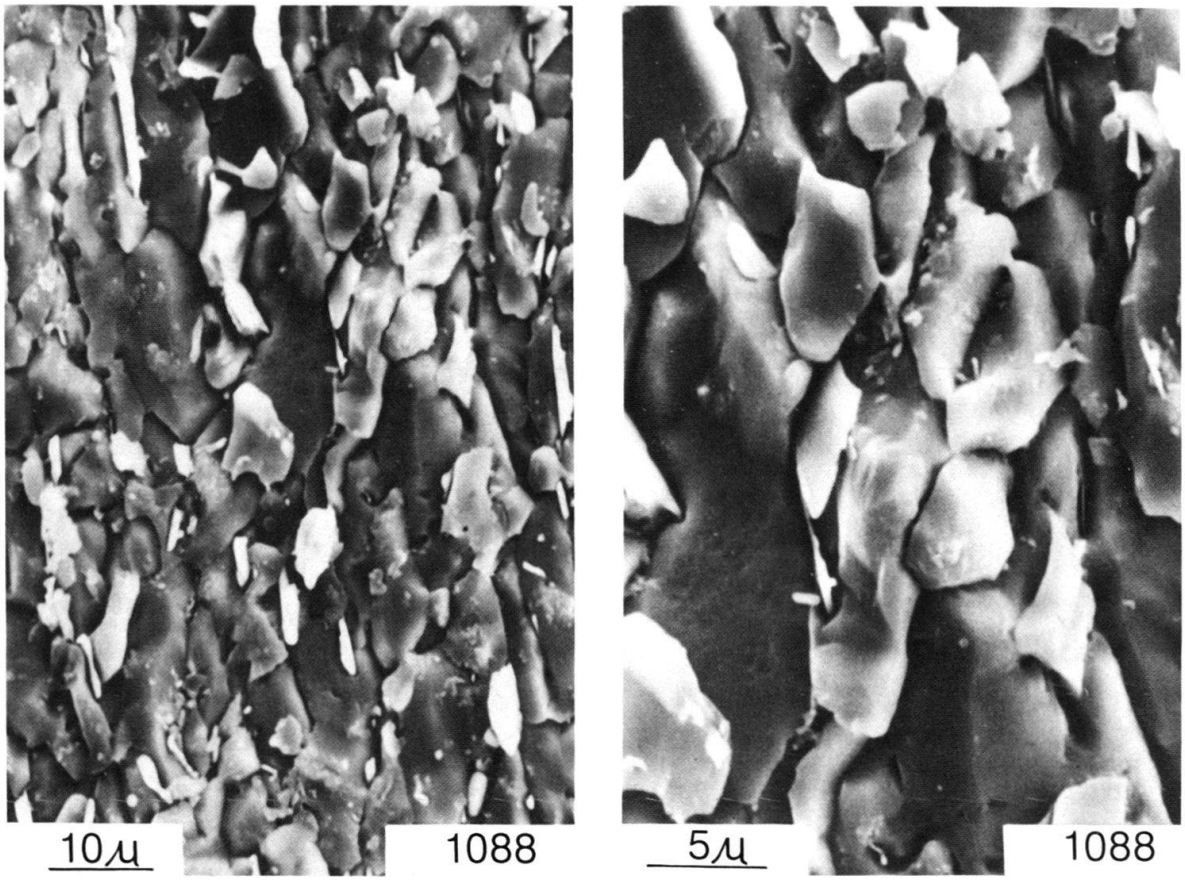

Fig. 12. SEM micrographs obtained from etched polished surfaces showing typical microstructure of sample 1088 from the epimetamorphic Infrahelvetic complex. Note the increase in grain size and the shape preferred orientation as compared to Figs. 5 and 9.

a pattern, which if compared to naturally deformed rocks (Schmid et al. 1981) and to experimental work (Schmid et al. 1987), is typical for rocks deforming with a component of simple shear in the regime of mechanical twinning. The sense of shear is sinistral, as indicated in the stereoplot in Fig. 11. As discussed by Schmid et al. (1987), the absence of twins in the calcite grains is at odds with textures indicating that deformation occurred in the twinning regime (their samples were from the very same fold). Despite this uncertainty, the similar textures at the various sites in the fold of sample 1088 suggest a homogeneous ductile shear that post-dates and overprints buckling.

Discussion and conclusion

The three fold structures investigated all have in common a structural setting characterized by large-scale folds associated with a basal detachment. One of the interesting questions is whether the outcrop-scale folds underwent layer-parallel shortening prior to buckling. Such a kinematic sequence has been reported from theoretical considerations and field data (Sherwin & Chapple 1968, Parrish 1973, Hudleston & Holst 1984). In the case of the Jura Mountains, layer-parallel shortening indeed occurred in an early stage of the folding process, i.e., prior to buckling. It is expressed

by partly conjugate reverse faulting ("wedging") affecting the mechanically stiff limestone layers. In contrast to folds in the Jura Mountains, the folds analysed in the Helvetic Zone lack indications of this early layer-parallel shortening. In fact, the textures in the folds from the Infrahelvetic complex suggest that the folds underwent passive simple shear after buckling. A study of folded oolitic limestones from the same general area in the Infrahelvetic complex (PFIFFNER 1980) indicates a homogeneous shear more or less coeval with buckling. However, for still other folds from this area, twinning strains suggest an early phase of a few percent of layer-parallel shortening (GROSHONG et al. 1984).

The development of reverse faults restricted to a single competent layer requires the presence of a local detachment horizon. In the example from the Jura Mountains, marly layers with a thickness of a few centimeters separating limestone layers with thicknesses of 5–20 cm were sufficient to serve as such horizons. The lack of true marly layers in the examples from the Helvetic Zone and the onset of folding at higher p-T conditions may be responsible for the suppression of reverse faulting during layer-parallel shortening in the early stages of the deformation.

The three samples investigated in this paper show a dramatic change in the active deformation mechanisms as a function of varying p-T conditions. In the Jura Mountains, which are in the zone of diagenesis, brittle features dominate at the small scale but cataclasis is able to produce fold structures which have to be considered ductile when viewed at a larger scale. As discussed by LAUBSCHER (1979), mass transport implies the movement of rigid blocks by means of slip on multiple sets of fault surfaces, pressure solution and dilation. The folds from the anchizonal Helvetic Nappes also have the macroscopic appearance of ductile flow, yet they deformed entirely by pressure solution and fracturing. The geometry and ductility therefore are not diagnostic of the actual operating deformation mechanisms. The fold of sample 1072 also suggests that substantial volume losses (up to 23%) are associated with folding. Here, pressure solution and fracturing associated with buckling define tangential-longitudinal intrabed strains with stretching parallel to bedding in the outer arc and shortening in the inner arc. For the epizonal Infrahelvetic complex, evidence for intracrystalline plasticity exists and explains some of the high strains associated with the observed folds. Conflicting evidence from measured textures (indicating a twinning regime) and observed microstructures (indicating dislocation creep) is not fully understood. But the lack of brittle features suggests that folding initiated by intracrystalline plasticity at elevated temperatures was not preceded by brittle deformation at low temperature. Although no features indicative of volume loss could be found in the folds of sample 1088, volume losses on the order of 10–30% were reported from oolitic limestones (PFIFFNER 1980) from the same general area and imply mass transport via a fluid phase.

Acknowledgments

This paper benefitted from comments by M. Burkhard, St. Schmid, X. Tschanz and M. Handy, who also corrected my English. I thank St. Schmid for the texture goniometry measurements, S. Huon and the Metallurgical Institute of the University of Neuchâtel for the preparation of the SEM micrographs, and I. Blaser for technical assistance. Financial support from grant 2.837–0.85 of the Schweizerischer Nationalfonds is acknowledged.

REFERENCES

ANGELIER, J. 1977: La reconstruction dynamique et géométrique de la tectonique de failles à partir de mesures locales (plans de faille, stries, sens de jeu, rejets): quelques précisions. C.R. Acad. Sci. Paris, Sér. D/285, 637–640.

BUXTORF, A. 1916: Prognosen und Befunde beim Hauensteinbasis- und Grenchenbergtunnel und die Bedeutung der letzteren für die Geologie des Juragebirges. Verh. Natf. Ges. Basel 27, 185–254.

DROXLER, A. & SCHAER, J.-P. 1979: Déformation cataclastique plastique lors du plissement sous faible couverture, de strates calcaires. Eclogae geol. Helv. 72, 551–570.

GROSHONG, R.H., PFIFFNER, O.A. & PRINGLE, L.R. 1984: Strain partitioning in the Helvetic thrust belt of eastern Switzerland from the leading edge to the internal zone. J. Struct. Geol. 6, 5–18.

HUDLESTON, P.J. & HOLST, T.B. 1984: Strain analysis and fold shape in a limestone layer and implications for layer rheology. Tectonophysics 106, 321–347.

LAUBSCHER, H.P. 1979: Elements of Jura kinematics and dynamics. Eclogae geol. Helv. 72, 467–483.

MILNES, A.G. & PFIFFNER, O.A. 1977: Structural development of the Infrahelvetic complex, Eastern Switzerland. Eclogae geol. Helv. 70, 83–95.

MOORE, C.H. 1989: Carbonate Diagenesis and Compaction. Developments in Sedimentology 46. Elsevier Science Press.

PARRISH, D.K. 1973: A nonlinear finite element fold model. Amer. J. Sci. 273, 318–334.

PERSOZ, F. & REMANE, J. 1973: Evolution des milieux de dépôt au Dogger supérieur et au Malm dans le Jura neuchâtelois méridonal. Eclogae geol. Helv. 66, 41–70.

PFIFFNER, O.A. 1978: Der Falten- und Kleindeckenbau im Infrahelvetikum der Ostschweiz. Eclogae geol. Helv. 71, 61–84.

— 1980: Strain analysis in folds (Infrahelvetic complex, Central Alps). Tectonophysics 61, 337–362.

— 1981: Fold-and-thrust tectonics in the Helvetic Nappes (East Switzerland). In: Thrust and Nappe Tectonics (Ed. by MCCLAY, K.R. & PRICE, N.J.) Geol. Soc. London Spec. Publ. 9, 319–327.

— 1982: Deformation mechanisms and flow regimes in limestones from the Helvetic zone of the Swiss Alps. J. Struct. Geol. 4, 429–442.

— 1986: Evolution of the north Alpine foreland basin in the Central Alps. In: Foreland Basins (Ed. by ALLEN, P.A. & HOMEWOOD, P.) Spec. Publs. int. Ass. Sediment. 8, 219–228.

PFIFFNER, O.A. & BURKHARD, M. 1987: Determination of paleo-stress axes orientations form fault, twin and earthquake data. Ann. Tect. I, 48–57.

PFIFFNER, O.A., KLAPER, E.M., MAYERAT, A.-M. & HEITZMANN, P. 1990: Structure of the basement-cover contact in the Swiss Alps. In: Deep structure of the Alps (Ed. by ROURE, F., HEITZMANN, P. & POLINO, R.) Mém. Soc. géol. France 156, Mém. Soc. géol. Suisse 1, Mém. Soc. géol. Italia, spec. Vol. 1, in press.

RAMSAY, J.G. 1967: Folding and Fracturing of Rocks. Mc Graw-Hill, New York.

RICKENBACH, E. 1925: Description du Val de Travers, du cirque de St. Sulpice et de la Vallée de la Brévine. Bull. Soc. Neuch. Sci. nat. 50, 1–76.

SCHMID, S.M., CASEY, M. & STARKEY, J. 1981: The microfabric of calcite tectonites from the Helvetic nappes (Swiss Alps). In: Thrust and Nappe Tectonics (Ed. by MCCLAY, K.R. & PRICE, N.J.) Geol. Soc. London Spec. Publ. 9, 151–158.

SCHMID, S.M., PANOZZO, R. & BAUER, S. 1987: Simple shear experiments on calcite rocks: rheology and microfabric. J. Struct. Geol. 9, 747–778.

SHERWIN, J.-A. & CHAPPLE, W.M. 1968: Wavelengths of single layer folds: a comparison between theory and observation. Amer. J. Sci. 266, 167–179.

SUPPE, J. 1985: Principles of Structural Geology. Prentice-Hall, London.

SUPPE, J. & MEDWEDEFF, D.A. 1990: Geometry and kinematics of fault-propagation folding. Eclogae geol. Helv. 83, 409–454.

Manuscript received 26 February 1990
Revision accepted 28 May 1990